PHYSICAL AND MECHANICAL PROPERTIES OF FOAMED PORTLAND CEMENT COMPOSITE CONTAINING CRUMB RUBBER FROM WORN TIRES.

J.N. Eiras[1], F. Segovia[2], M.V. Borrachero[1], J. Monzó[1], M. Bonilla[1], J. Payá[1]

[1]Instituto de Ciencia y Tecnología del Hormigón. Universitat Politècnica de València. Camino de Vera s/n, Edificio 4G, 46022 València. Spain.

[1]Instituto de Tecnología de Materiales. Universitat Politècnica de València. Camino de Vera s/n, Edificio 5E, 46022 València. Spain.

*Corresponding author: jeseifer@posgrado.upv.es

Abstract

The management of worn tires is a concern in industrialized countries. The application of crumb rubber as lightweight aggregate in cement based materials is a green alternative for reusing this material, and it is more interesting than energy recovery from an ecological point, regarding the waste hierarchy. High replacements of natural sand by crumb rubber were studied, and an air-entraining agent was employed in order to achieve a cellular structure in the composite. The obtained results from tests in fresh state reveal an improvement in workability. The tests conducted on hardened composite reveals promising properties that postulate the resulting materials as candidate for applications where thermal and acoustic properties are required. The minimum requirement of mechanical strength for masonry units was also achieved since the obtained compressive strength varies between 1.04 to 10.04 MPa. Finally, potential applications as a construction material have been highlighted for civil and building applications.

Keywords: Crumb rubber, rubberized mortar, cement based composite, air-entrained.

1. Introduction

Nowadays, the management of worn tires needs creative solutions to reduce the volume of tires that are generated year after year since they cannot be stored in stockpiles. Improper disposal or production of large amounts can seriously pollute the environment. The solutions adopted worldwide include: i) reuse tires through selling retreaded and second-hand ones, ii) material recovery from whole, chopped, shredded and micronized tires and finally, iii) energy recovering. Following this order, the well known waste hierarchy is particularized for the management of worn tires. It reflects several ways of the management of worn tires prioritizing them from highest to lowest in ecological quality. Nevertheless, the quantity consumed in material recovery applications is lower than those generated at almost all industrialized countries which already manage close to 100% of the generated tires each year, the excess of tires that is not consumed by material valorization applications is used as energy recovery. In Spain, in 2011, 42% of worn tires generated have been destined to energy recovery, mainly in cement kilns; 10% have been reused and 48% have been materially recovered [1]. Since incineration of worn tires by partial replacement of natural sources can be discussed due to the increase in emissions to the atmosphere as solid particles, metals, CO, SO_2 and HCl, it is necessary complementary material valorization solutions which could be interesting from an ecological point of view.

Material recovery of worn tires in cement based materials as aggregate has been broadly studied [2-4]. Observations made on rubberized concretes and mortars against plain ones, concluded that workability, fresh unit weight, and dry bulk density decreases as a measure that rubber content increases [5-6]. In all cases researchers have identified a loss of mechanical strength and static modulus either flexural, compression or tensile even by using fibers [4,7-9]. This effect can be attributed to the lack of adherence between rubber and cement matrix [10]. Adherence has attempted to be improved after rubber pretreatment by chemical attack and by using silanes [11-14]. Except in studies carried out by Segre et al. and Rostami et al., rubber pretreatment resulted ineffective and in addition, any pretreatment to rubber aggregates delays immediacy to use this waste.

Other properties studied on rubberized concretes and mortars drawn a decrease on thermal conductivity [15-17] and vibration attenuation [6, 17]. This promising composite also improves the freeze thaw resistance [18], chloride ion penetration [19], improves impact resistance [20], decreases the depth damage against fire [21] and increases the fracture toughness [2, 8-9]. Nevertheless, all properties studied depend on shape, size and comminuting process. Some kinds of rubber show better behavior for some properties than other ones. Najim and Hall [22] suggest the use of crumb rubber (CR) to other products because of better behavior to the losses of resistance and cost than chips, fibers and powder.

The aim of this work is to study the physical and mechanical properties of foamed mortars with CR as lightweight aggregate. Previous work was conducted by Benazzouk et al. on aerated rubber cement composites [23], but emphasis was not made on their thermal and acoustic behavior as well as their potential constructive applications.

2. Experimental

2.1 Materials

Mortar samples with a water/cement ratio (w/c) of 0.5 by weight and aggregate/cement ratio (a/c) of 3.83 by volume were prepared. The Portland cement employed was CEM I

52.5R with a density of 3.10 g/cm^3. Crumb rubber (CR) from mechanical shredding of worn tires, with maximum size of 2.2 mm and fineness modulus of 3.90, was employed in mortar mixtures by partial substitution of siliceous aggregate (natural sand), with fineness modulus of 3.10. The density obtained for both aggregates were 1.15 and 2.43 g/cm^3 respectively. The particle size distributions for aggregates used in this work are shown in Fig.1.

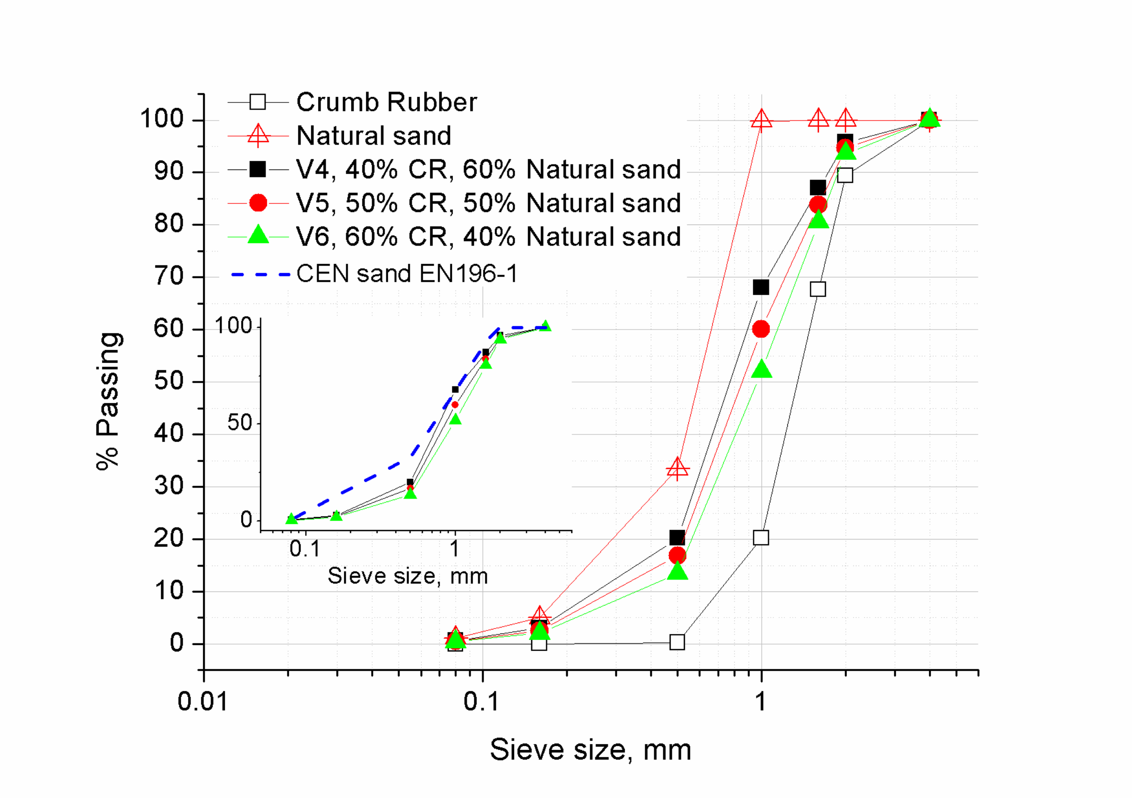

Figure 1. Particle size distributions for CR and natural sand.

Replacement ratios in volume, of natural sand by CR were studied at 40, 50 and 60 % levels (replacement levels: V4, V5 and V6). The air entraining agent (AEA) used was Genapol PF80 Powder, that is a low-foaming, non-ionic surfactant. It was added in amount of 0.125, 0.250, 0.500, and 0.750 % by weight of cement to achieve a lightweight composite and a porous structure (AEA levels: T1, T2, T5 and T7). Furthermore, control dosages without any AEA were prepared by using a sulphonated melamine based superplasticizer Melment L10/40. It was added in amount of 1% by weight of cement, for all replacement levels of natural aggregate by CR (K series mortars: V4K, V5K and V6K). Finally, a standard Portland cement mortar (MS) was prepared as reference material following the standard EN-196-1 [24]. The Table 1 summarizes the working levels employed in this study. A number of three samples per type of mortar were prepared.

Table 1. Working levels

CR			V4	V5	V6
			40%	50%	60%
Superplasticizer		1.000%	V4 K	V5 K	V6 K
AEA	T1	0.125%	V4T1	V5T1	V6T1
	T2	0.250%	V4T2	V5T2	V6T2
	T5	0.500%	V4T5	V5T5	V6T5
	T7	0.750%	V4T7	V5T7	V6T7

2.2 Tests procedures

The flow table test was performed on the fresh batches in accordance with EN 1015-3 [25]. Prismatic 40 mm x 40 mm x 160 mm test samples were confectioned and preserved in a moist chamber at 20ºC and 95% of relative humidity for 28 days. After curing, they were saturated for 24 hours in water to determine the saturated weight mass. The dry bulk density is also ascertained by weighting, after drying the samples at 60°C until constant mass is reached. Once the specimens were dried, ultrasonic pulse velocity by direct transmission in accordance with ASTM C 597 [26] were determined with a TICO ultrasonic instrument. The fundamental transverse frequency test (ASTM C 215 [27]) was conducted. The excitation of resonance frequencies were achieved by dropping an alumina ball with mass of 3.25 g from a distance of the sample of 10 cm.

The excitation was sensed with an accelerometer (PCB with sensitivity of 0.956 mV/ (m.s^{-2}). A total of 8192 points were recorded with a sampling frequency of 25 kHz. Ten impacts per sample were recorded and transformed to the frequency domain with the FFT algorithm. Finally, the mechanical strength was obtained in the displacement control environment at a rate of 1 mm/min in an INSTRON universal testing machine (model 3382). Undisturbed fragments were extracted from test samples to exam by Scanning Electron Microscopy (SEM). Moreover, V4T5, V5T5 and V6T5 mortars were selected to prepare 150 mm x 150 mm x 20 mm specimens, to determine their thermal conductivity, with a thermal conductivimeter NEOTIM FP2C, based on hot-wire technique.

3. Results and discussion

3.1 Consistency of fresh mortar

The mortars were targeted in function of their slumped cone diameter as fluid, plastic or dry consistency in accordance with EN 1015-3 [25]. Then, it is necessary to add superplasticizer in rubberized mortars without AEA i.eV4K, V5K and V6K, in order to achieve workable mortars. The batches classified as dry consistency mortars presented the formation of 0.5-1.5 mm balls during the compaction. This phenomenon is not desirable in practice, and it can be avoided by increasing the w/c ratio, or by using superplasticizers. However, when the amount of water or superplasticizer dosage is increased, mortar segregation and bleeding can be caused. In particular, Turatsinze et al. combined different superplasticizers and air entraining agents to prevent segregation and bleeding on rubberized concrete [8].

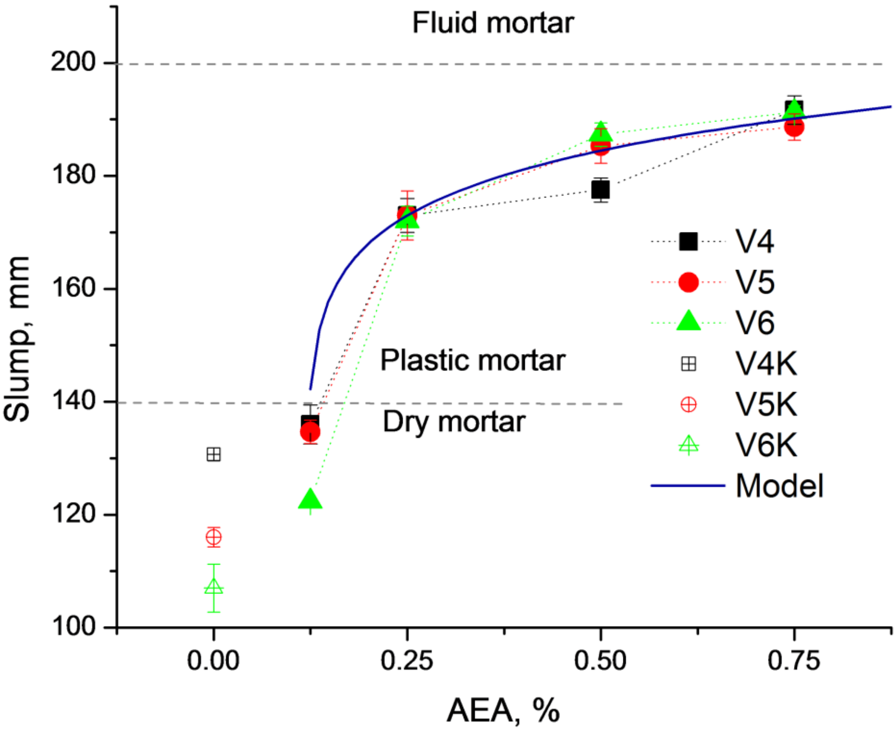

Figure 2. Slump of mortars versus AEA content.

The flow table tests results obtained versus the AEA content are represented in the Fig. 2. The greater AEA content the higher workability. All CR contents studied (40, 50, 60%) follow the same behaviour regardless their CR content. The results have been fitted to the potential model (Eq.1).

$$\Delta S = a + (AEA - b)^{c} \qquad (1)$$

Where ΔS is the difference between the slumped cone diameter before and after complete 15 shocks, AEA is the air entraining agent in percentage and *a*, *b* and *c* are fitting parameters. This model has been fitted for all CR contents studied since there are not significant differences between them. The proposed model can approach the behavior of any additive used in cement based materials to determine their effectiveness through the interpretation of the parameters *a*, *b* and *c*. The exponent *c* reveals the degree of curvature of the function and *b* is the vertical asymptote value that defines the theoretical minimum AEA content to obtain workable mortar. The obtained fitting parameters were found *a*=96.067, *b*=0.125, *c*=0.136 with a coefficient of determination R^2=0.97.

The ability to generate air bubbles increases with increasing AEA content in the mortar, since the AEA reduces its viscosity and consequently, the air generated can easily move into the fresh mortar to form large bubbles from small ones. Therefore, the rheological properties can directly affect the air-void system. In Fig. 3a and 3b are represented the lateral surfaces of samples V4T1 and V6T7 respectively. Qualitatively, it can be observed that there are larger pores constituted on the walls of the samplesT7, with greater workability, than in samples T1 which show the inherent porosity due to a poor compaction.

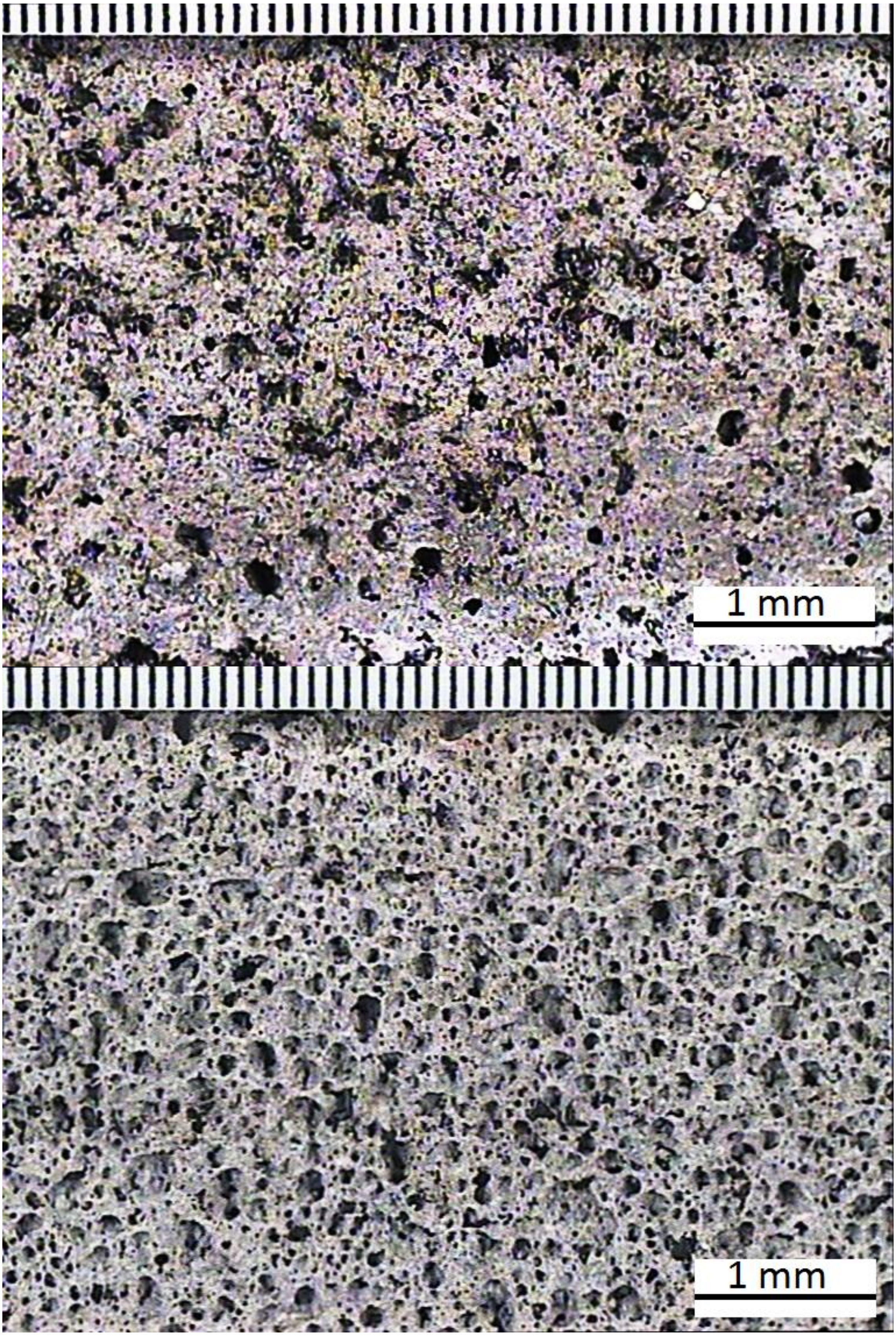

Figure 3.Lateral surfaces of samples a)V4T1 and b)V6T7.

3.2 Dry bulk density and absorption in percentage

After weighting saturated and dry specimens, absorption (in percentage) and dry bulk density can be obtained. The results obtained are represented in Fig. 4a and 4b.They show that dry bulk density decreases with increasing the replacement of siliceous aggregate by CR since the density of the siliceous aggregate is close to twice CR density, and also decreases with increasing AEA content. In all cases, the dry bulk densities were lower and the absorption values were higher than those obtained for the reference standard mortar (MS). The absorption does not change significantly with CR for K series mortars (V4K, V5K and V6K) and T1 series mortars (V4T1, V5T1 and V6T1). However, for greater percentages of AEA, the greater amount of CR, the greater absorption percentage. Therefore, the mortars with greater CR content are able to incorporate more air as a measure that the AEA increases, which implies an increase in connected porosity and hence water absorption in percentage.

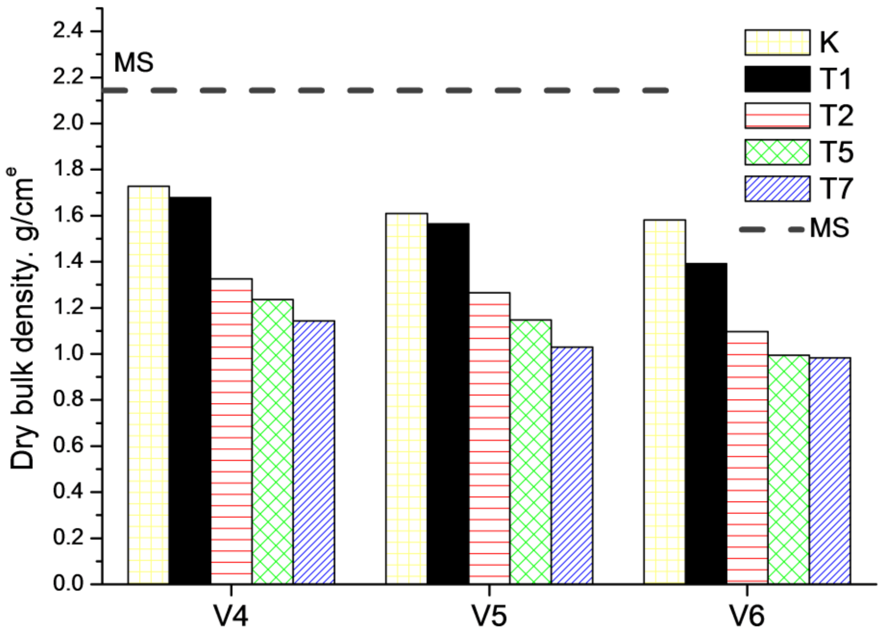

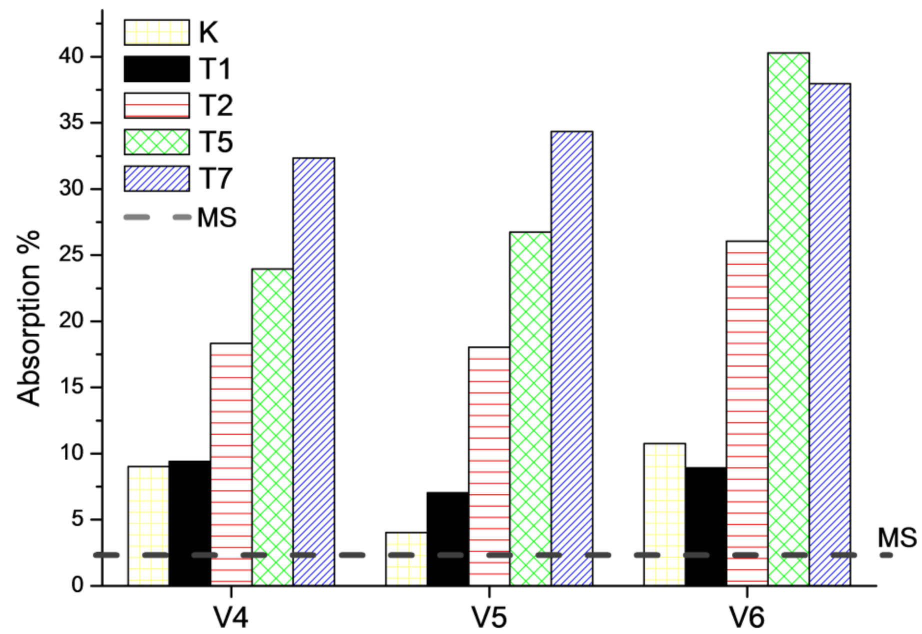

Figure 4. a) Dry bulk density, b) Absorption in percentage. Dashed lines represent the properties of standard cement mortar (MS).

The results are in agreement with a previous research that reported greater amounts of air in concrete with rubber control concrete [3, 7]. Siddique et al. note that this effect may be due to the non-polar nature of rubber and its tendency to entrap air in their rough surface [10].

3.3 Mechanical properties

In the Table 2 are listed the results for both flexural and compressive strengths. The results show that the incorporation of AEA and CR cause losses on the mechanical strength, either compressive (Rc) or flexural strength (Rf). Although Toutanji et al. [28] point out that the loss of flexural strength is lesser in magnitude than the compressive strength, large volumes of aggregate replacement by CR and the incorporation of AEA, equal both detriments. For example, the reduction in flexural and compressive strength of mortar V4T2 respect to the plain mortar MS is 90.5% and 92.2% respectively.

Table 2. Mechanical properties for mortars: Flexural (Rf) and compressive (Rc) strength

Mortar	**Rf, MPa**	**Rc, MPa**
MS	10.86 ± 1.38	52.13 ± 2.29
V4K	2.50 ± 0.05	11.55 ± 0.74
V4T1	1.81 ± 0.29	10.04 ± 0.45
V4T2	1.03 ± 0.02	4.08 ± 0.24
V4T5	0.71 ± 0.07	2.89 ± 0.14
V4T7	0.48 ± 0.01	1.91 ± 0.12
V5K	2.22 ± 0.18	10.57 ± 0.57
V5T1	1.78 ± 0.05	8.45 ± 0.31
V5T2	0.75 ± 0.08	3.18 ± 0.08
V5T5	0.50 ± 0.09	1.84 ± 0.07
V5T7	0.47 ± 0.09	1.38 ± 0.21

V6K	1.21 ± 0.75	5.80 ± 0.35
V6T1	1.12 ± 0.08	4.13 ± 0.20
V6T2	0.47 ± 0.01	1.32 ± 0.05
V6T5	0.35 ± 0.00	1.09 ± 0.05
V6T7	0.27 ± 0.07	1.04 ± 0.06

The loss of strength is associated to the poor interface between CR and the cementing matrix. In the Fig. 5a and 5b are shown the fracture surfaces of mortars V4T2 and V4T5 respectively. It can be noticed the low presence of rubber particles in the fracture surface of the V4T5 specimen. This is due to the greater amount of AEA causes i) an increase in the volume of paste, so that the ratio dispersed phase (CR) to matrix decreases despite having the same proportion in the dosage and ii) a greater loss of adhesion of the particles due to the increased incorporation of air.

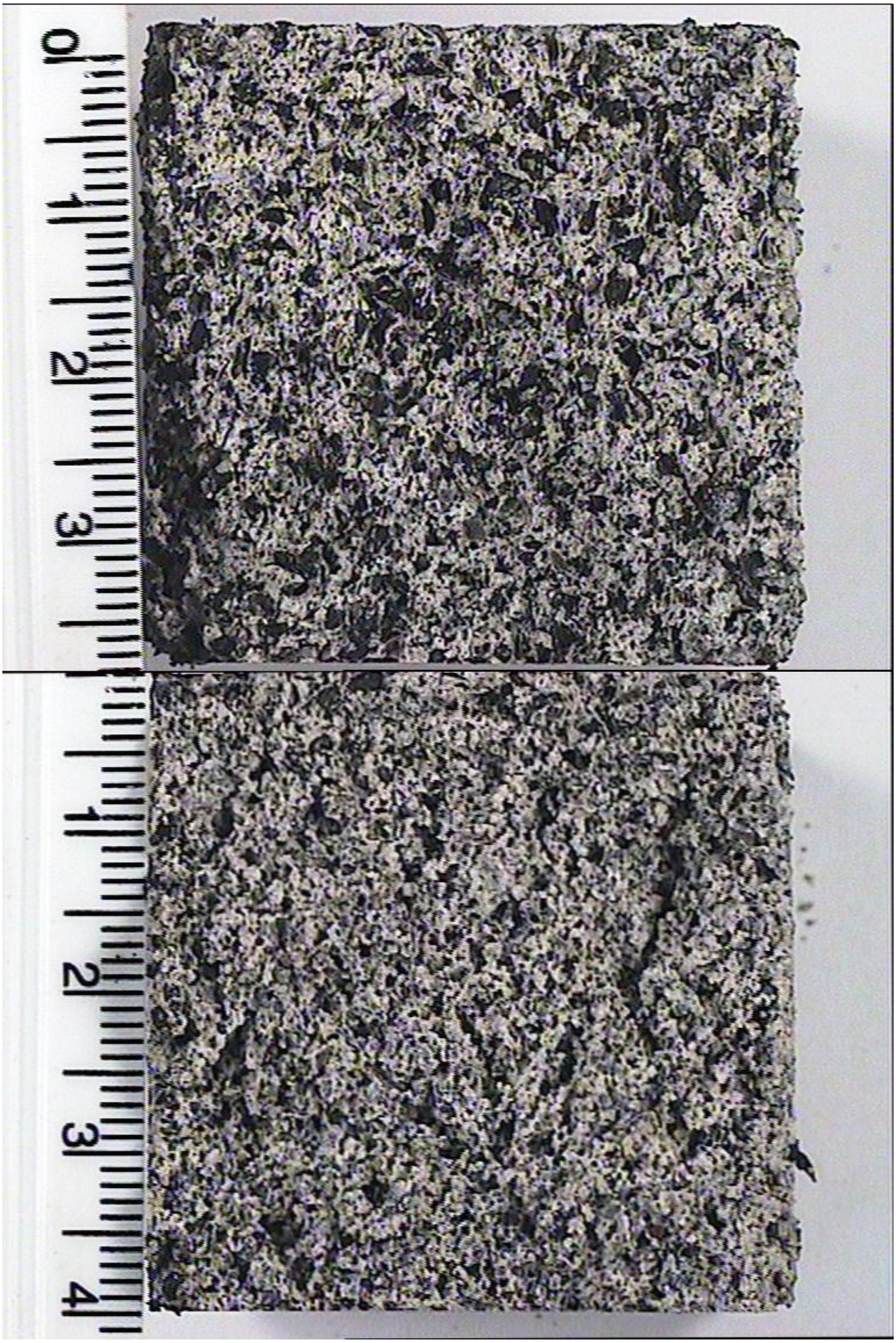

Figure 5. Flexural fracture surfaces of mortars a) V4T2 and b) V4T5.

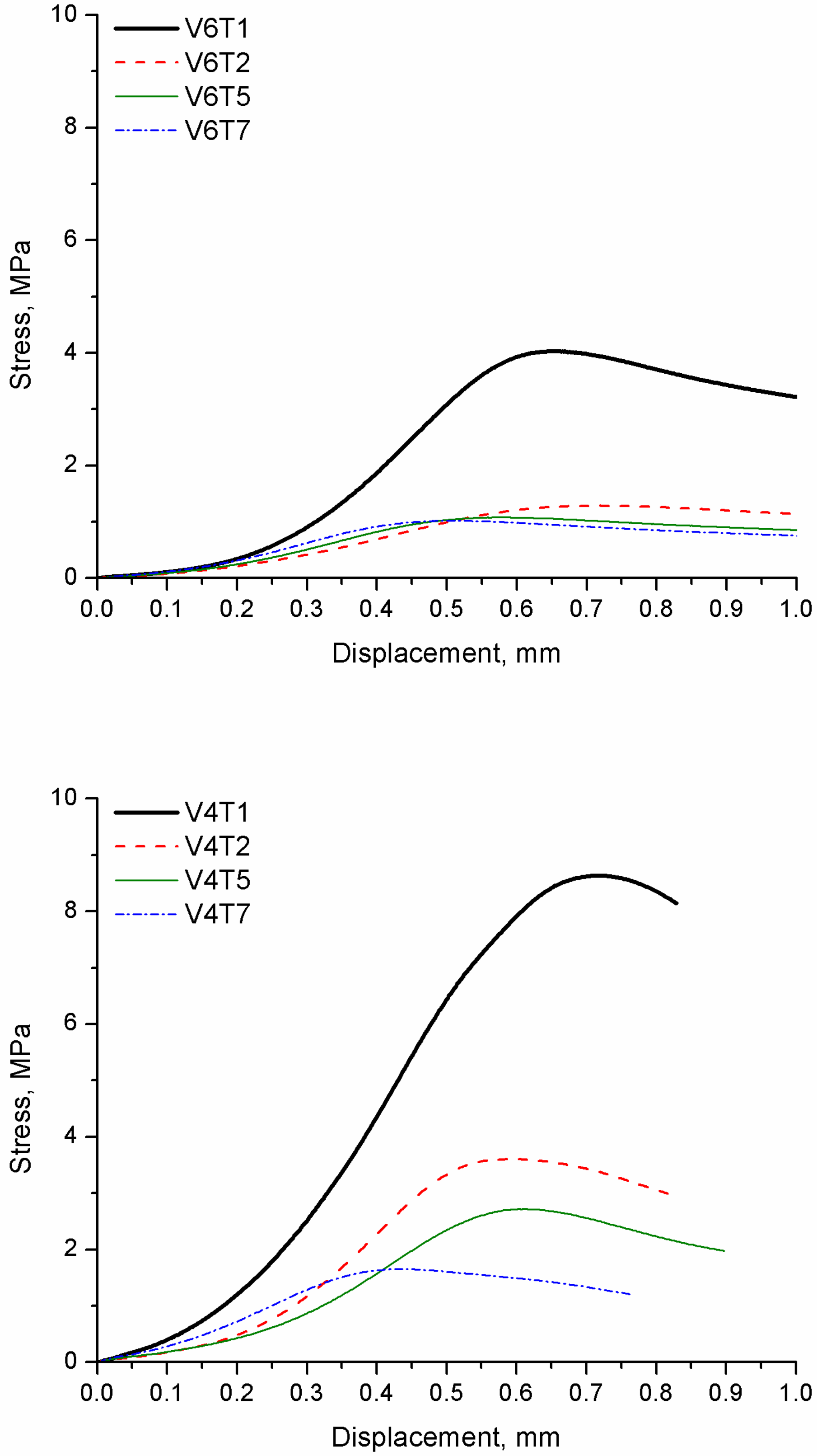

Figure 6. Compressive stress versus displacement for mortars with AEA, a) seriesV4, b) series V6.

In Fig. 6 are represented the curves of compressive stress versus displacement of all mortars containing AEA. Qualitatively, we can observe a decrease in the elastic modulus and a decrease in the slope after maximum stress, indicating a progressive increase in the capacity to bear strength after the maximum compression strength with increasing AEA and with increasing CR. We have estimated the static modulus by linear regression in the elastic range on the stress-displacement curves [29]. The values are listed in Table 3. By means of the ultrasonic wave velocity through the prismatic samples (V), the dynamic elastic modulus (Ed_{upv}) can be obtained (Eq.2), knowing the density ρ and assuming in our case a Poisson's ratio (ν) of 0.3 [30].

$$Ed_{upv} = V^2 \cdot \rho \cdot \frac{(1+\nu)\cdot(1-2\nu)}{1-\nu} \qquad (2)$$

Moreover, the dynamic bending modulus of elasticity can be also obtained from the fundamental transverse frequency test (Eq.3), knowing the density (ρ), the length (L), the radius of gyration (t) of the sample and the resonance flexural frequency (F_f).

$$\mathrm{Ed_{ff}} = \frac{4\pi \cdot L^4 \cdot F_f^2 \cdot \rho 1.401}{4.73^4 \cdot t^2} \qquad (3)$$

The dynamic modulus of elasticity is commonly related to the compressive strength and static modulus and different expressions have been provided [31-32]. We find a linear relationship between the estimated static modulus (Es) and the dynamic elastic modulus either, from ultrasonic wave velocity (Ed_{upv}) or from fundamental transverse frequency (Ed_{ff}), indicating that both dynamic modulus are good estimators of static modulus in the rubberized mortars studied (Fig.5)

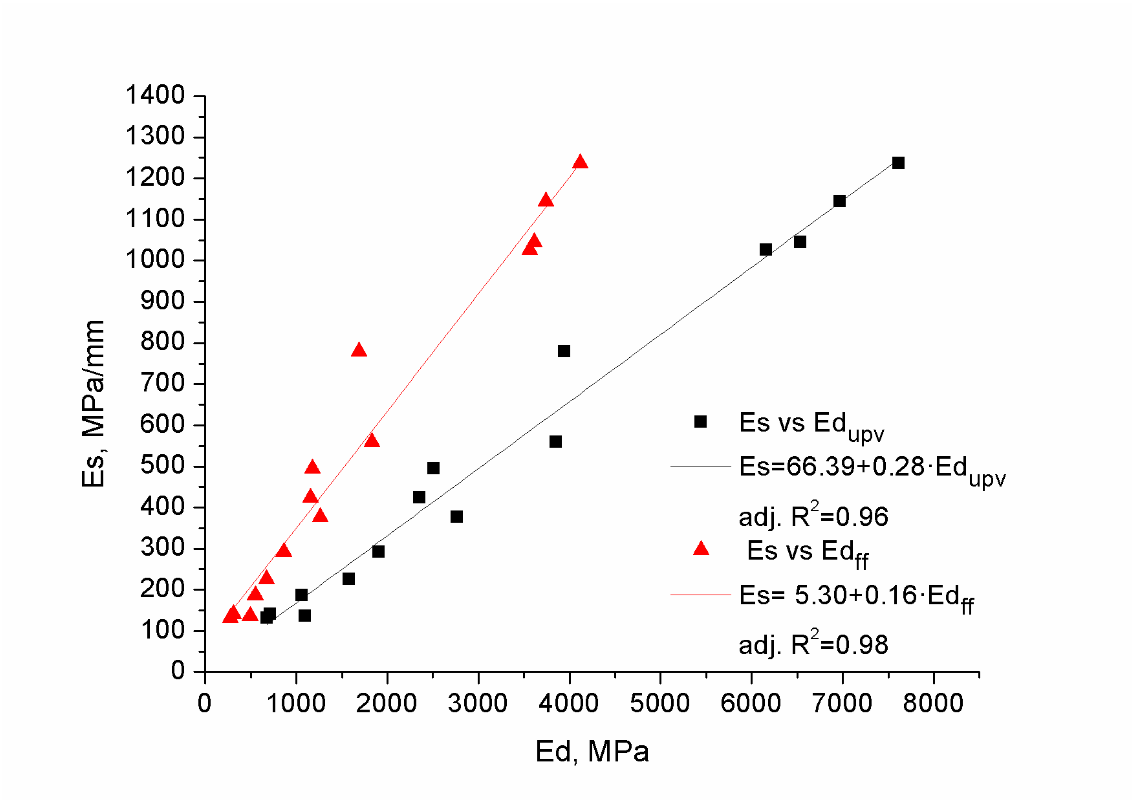

Figure 7. Static modulus in function of dynamic modulus of elasticity.

When results obtained for plain mortar (MS) are compared to those obtained for aerated rubberized mortars, it can be appreciated a greater reduction of stiffness. For example the Ed_{upv} obtained for MS is 34.56 GPa while for the weaker mortar in this study (V6T7 is Ed_{upv}=0.71 GPa. The aforementioned methods to compute the dynamic modulus of elasticity [26-27] are valid when isotropic, homogeneous and perfectly elastic materials hypothesis can be made [33], which are applicable to conventional concrete and mortar [32] but the present composites have discontinuities and heterogeneities, such as the incorporation of AEA and CR, that are the main responsible of great reduction of stiffness. Bridging the gap between damage under uniaxial compression, and the damage induced by incorporating of air bubbles and CR, the loss of mechanical properties, as a measure that CR and AEA increases, can be addressed by means of the relation between velocities, also known as continuity index (CI_v). It was proposed by Gorisse [34] to take into account discontinuities in the material, after normalizing the ultrasonic velocity values, with the ultrasonic velocity in the reference material [30, 35]. In this study, the CI_v has been computed using, the velocity obtained for MS, V_o=4203.15 m.s^{-1} as reference value. Analogously to CI_v, the continuity index can be expressed through fundamental flexural frequency (CI_f), when normalizing the frequency by the measured for the standard mortar MS (f_o=5282.78 Hz). Both computed continuity indexes for each mortar, either CI_v or CI_f, are related to the loss of mechanical strength as can be seen in Fig. 6. The compressive strength (Rc) was found to be related to the continuity index (CI) in the form (Eq.4):

$$Rc = r \cdot e^{(s \cdot CI)} \tag{4}$$

Where the fitting parameters were found to be r=0.22 and s=6.80 for CI_v and r=0.41 and s=6.96 for CI_f.

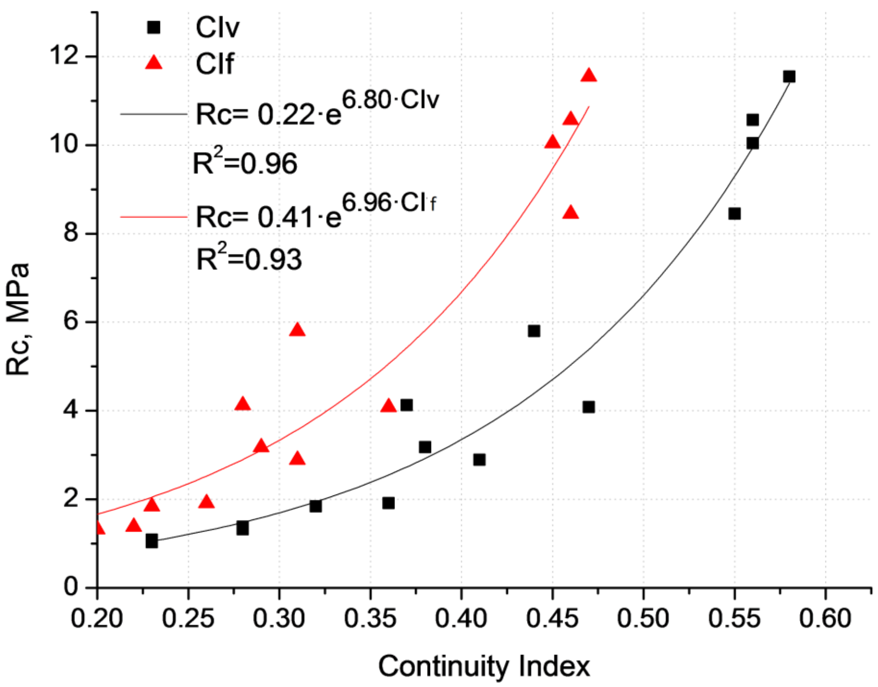

Figure 8. Compressive strength as function of CI

3.4.2 Damping properties

The vibrations through the samples are accompanied by a loss of energy due to internal friction. In consequence, the amplitude of vibration decreases, and the energy dissipated increases with time. This effect has been addressed through i) ultrasonic measurements and ii) the resonance test by means of the damping coefficient.

3.4.2.1 Attenuation coefficient in ultrasonic measurements

The ultrasonic resistance R_a was computed through the dry bulk density and the ultrasonic pulse velocity for each mixture. This method was previously attempted by Albano et al. in order to explore the attenuation properties on rubberized concrete [13]. Assuming that attenuation is produced uniformly, the attenuation coefficient α measured in decibels (dB) per percentage of CR (dB/%CR) can be through the model (Eq.5)

$$Ra = Rao \cdot e^{(-\alpha(CR))}, \quad (5)$$

where R_{ao} is the ultrasonic resistance for the reference material MS and CR is the percentage of CR. The Table 3 summarizes the mean and the standard deviation of ultrasonic pulse velocities, the obtained R_a grouped by AEA content, and the attenuation coefficient obtained by fitting the data to the aforementioned model. The obtained results show that the damping properties respect to the MS increase when CR increases. Moreover, the energy losses that implies the incorporation of CR depend on AEA content, as can be drawn of the computed values of α in dB/%CR.

Table 3. Ultrasonic pulse velocity, ultrasonic resistance and attenuation coefficient

	Es (MPa/mm)	**Ed_{ff} (ASTM C-215) (MPa)**	**Ed_{upv} (ASTM C597) (MPa)**
V4K	1235.90	4115.01	7619.26

V4T1	1143.97	3740.48	6968.33
V4T2	559.56	1830.86	3850.43
V4T5	376.91	1261.21	2769.69
V4T7	290.86	861.07	1905.40
V5K	1044.72	3612.39	6537.54
V5T1	1025.49	3562.27	6160.55
V5T2	423.73	1154.07	2353.20
V5T5	225.84	672.65	1580.87
V5T7	186.45	550.78	1059.50
V6K	778.65	1691.34	3946.37
V6T1	493.88	1177.98	2513.50
V6T2	135.62	494.37	1099.36
V6T5	131.92	278.65	676.24
V6T7	140.50	308.25	711.73

3.4.2.2 Vibration damping properties

In the Fig. 7, typical recorded time histories obtained in the fundamental transverse frequency test are displayed for mortars V4K, V4T2, V4T5 and V4T7. Damping coefficient computed through logarithmic decrement equation (Eq.6) can address the attenuation properties through the response signal in the time domain, where A_o and A_n are the initial amplitude and the amplitude value after *n* cycles respectively [36-39].

$$\varsigma_n = \frac{1}{(2n\pi)} \cdot \ln\left(\frac{Ao}{An}\right) \qquad (6)$$

The greater value of damping ratio, the more signal attenuation. Therefore high vibration damps are observed when increase the amount of CR and AEA, namely by increasing the number of discontinuities into the material. The damping coefficient has been calculated with a reference of 10 cycles in the time domain for each mortar (ζ_{10}). The results are shown in the Fig.8. The results reveal an increase in damping properties with increasing CR and AEA content. Similar results were reported by Najim and Hall [39] who found a linear relation between rubber content and damping coefficient in self-compacting concrete. The meaningful contribution of CR and AEA to damp vibrations can be better appreciated, when are compared to the damping coefficient obtained for MS, the damping coefficient obtained for aerated and rubberized mortars are between 2 and 4 times greater than those obtained for MS.

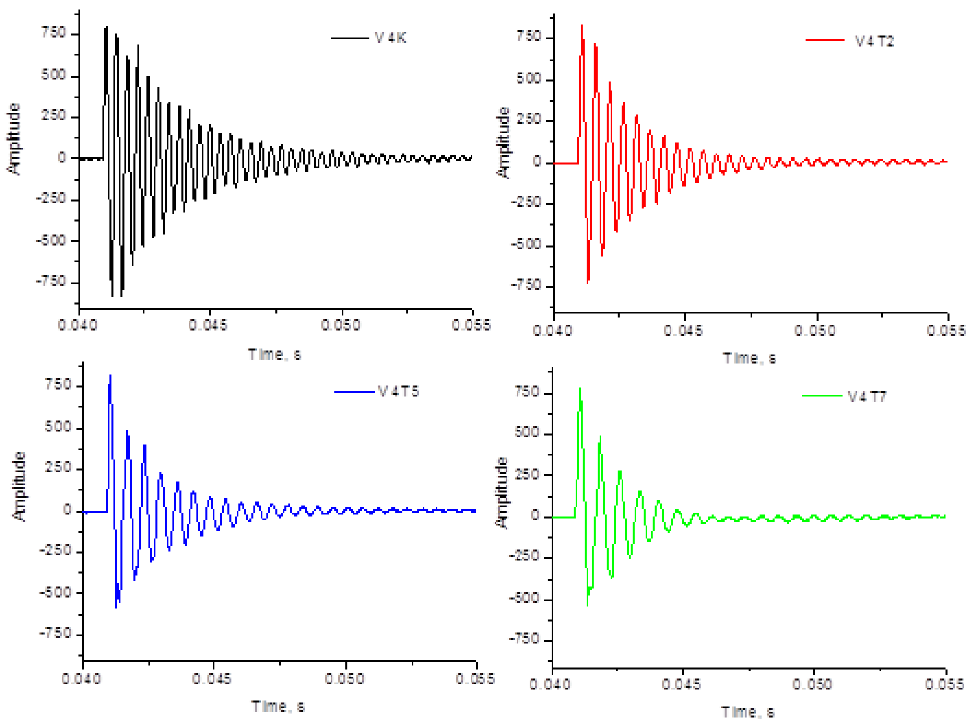

Figure 9. Typical signal responses in time domain for mortars V4K, V4T2, V4T5 and V4T7.

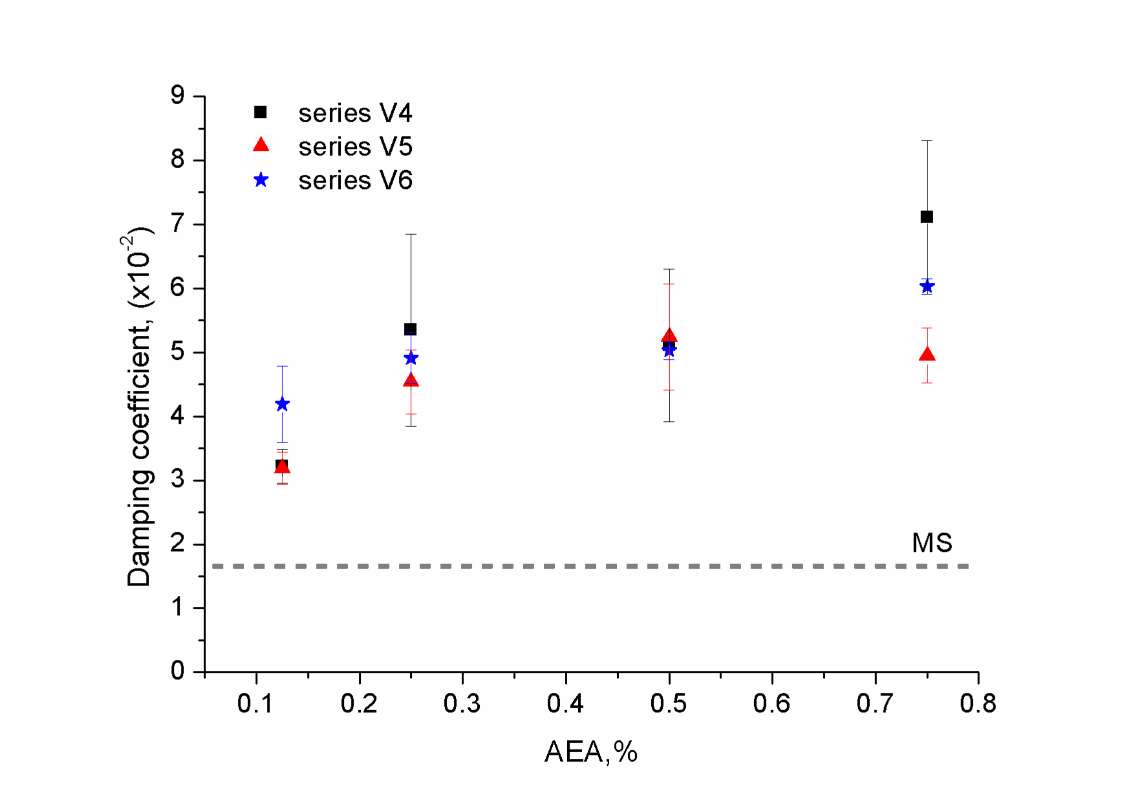

Figure 10. Damping factor after 10 cycles.

3.5 Thermal conductivity

The mortars with 0.500 % of AEA (mortars T5 series) were selected to determine their thermal conductivity (λ). The results listed in the Table 6 show that the thermal conductivity decreases with increasing CR content. The incorporation of rubber particles in the composition of the mortars and concretes reduces the thermal conductivity as the amount of rubber particles increases in its composition. This is due to the difference in conductivity between the siliceous aggregate, 2.45 to 5.20 W / (m.K), and CR, varying from 0.25 to 0.50 W / (m.K). However, the thermal conductivity does not depend exclusively on the conductivity of its constituents, but also its network of pores, moisture content, degree of crystallization, its cellular structure, etc. [40-41]. Research conducted by Hall et al. [42] drawn that the ability of rubber aggregates to entrap air is beneficial to obtain low-thermal conductivity in rubberized concrete.

Table 6. Thermal conductivity from hot-wire tests. Mean values and their standard deviation.

	Batch Id	ρ (Kg/m^3)	λ (W/mK)	Type
Paine et al. [38]	"Rubcrete"	1190	0.300	Concrete
Paine and Dhir [27]	25% GR1 (by mass)	1000	0.300	Concrete
Sukontasukul [25]	6CR30	2030	0.241	Concrete
Bennazouk et al.[23]	50%	1150	0.470	Mortar

The results show that increasing the CR dosage decrease the thermal conductivity of mortars, reaching values of conductivity lower than conventional concrete (λ=1.5-0.97 W / (m.K)) and similar products on the market currently available as concrete with expanded clay (λ=0.76-0.27 W / (m.K)) [45]. In the Table 7, the thermal conductivity results are compared to those found by other researchers in concrete that incorporates rubber aggregates.

Table7. Comparison of thermal conductivity obtained by other researchers in rubberized concrete and mortar.

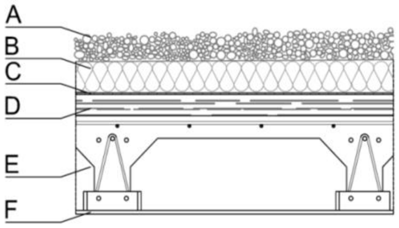

Layer		Thickness (m)	Thermal Conductivity λ (W/mk)	Thermal resistance (m^{2}k/W)
A	Gravel	0.050	2.000	0.03
B	PS Isolation	0.030	0.034	0.88
C	Waterproofing	0.005	0.700	0.01
D	V6T5	0.100	0.250	0.40

E	Concrete slab with EPS vaults	0.300	0.500	0.60
F	Plaster	0.015	0.350	0.04
U		0.47 W/m^{2}K		

The results obtained in this study shows the positive synergy between the AEA and the air entrapment achieved by the CR which allows to obtain low-thermal conductivity materials.

3.6 Microstructure: SEM observations.

SEM micrographs show the interface transition zone (ITZ) for mortar V4T1 and mortar V4T7 in figures 9a and 9b respectively. Turki et al. point out that at least two types of porosity exists on rubberized mortars: i) those inherent to the Portland cement matrix and ii) those as consequence to use rubber aggregates [30]. This study reveals that the greater CR content, the greater air content is detected and CR is able to stabilize the bubbles into the fresh batch even at high levels of AEA. SEM observations confirm that the hydration products around the aggregates have different nature. Ettringite is preferably placed in cavities and large pores and it also surrounds aggregates at high levels of AEA. Given that ettringite is an expansive hydration product, we suggest that their origin on the vicinity of the CR can be due to movements of hydration products from high pressure zones to lower ones rather to a sulfate ion transfer from the CR as result of chemical attack.

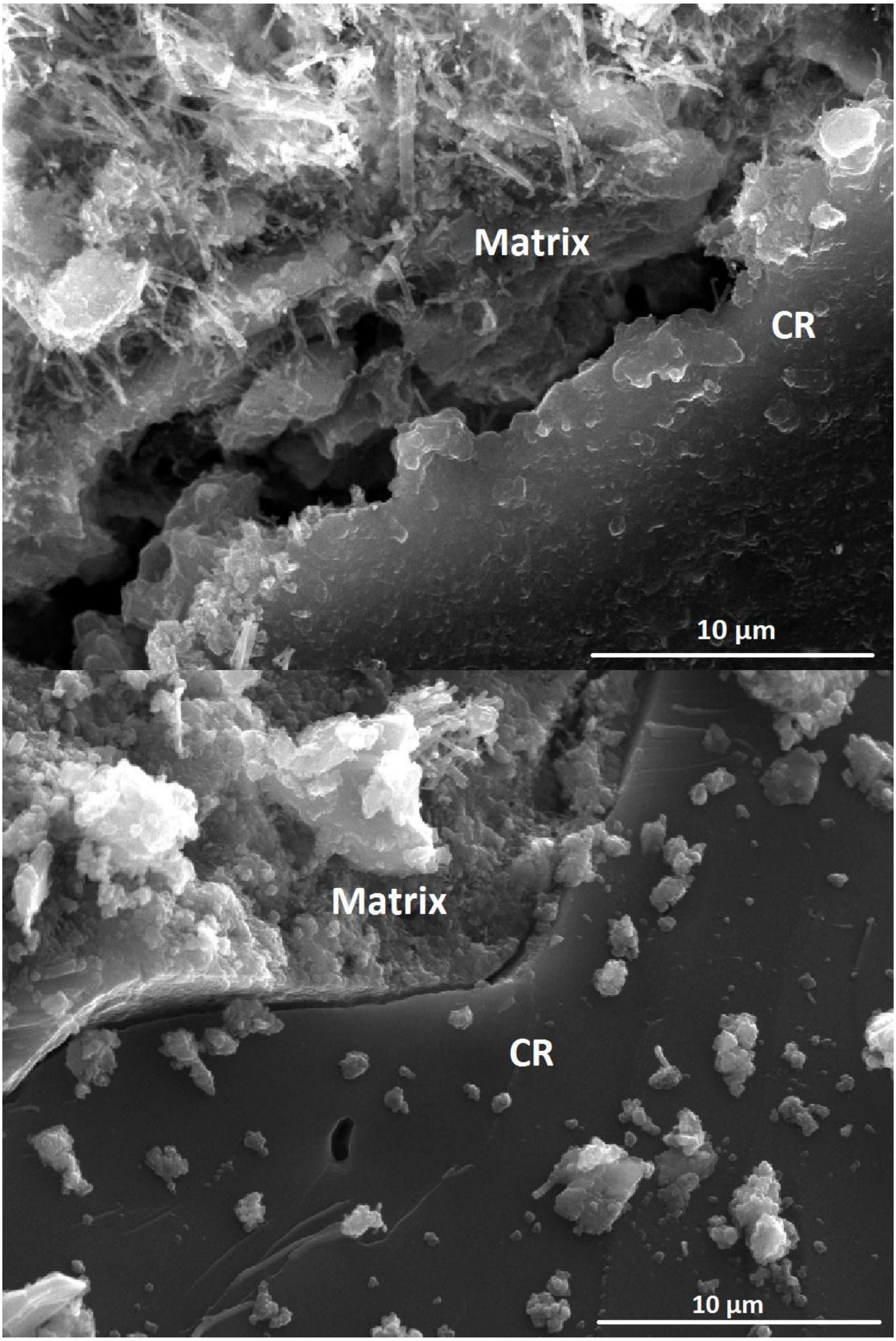

Figure 9. SEM micrographs for ITZ of mortars a) V4T7 (left) and b) V4T1 (right).

4. Concluding remarks

Non-structural applications are suitable for rubberized mortars. Thus, potential application to consider is as aggregate in foamed mortars. The promising properties obtained for aerated cement rubber composites suggest that there are several applications where the present material is suitable in basis to their properties i) mechanical strength, ii) damping properties, iii) thermal conductivity and finally iv) water permeability.

i) Mechanical strength

The compressive strength of the samples with AEA varies between 10.04 and 1.03 MPa, which relegates the application of these mortars mainly non-structural applications. However, the minimum strength required for masonry units is 2.5 MPa and 5.0 MPa for clay and calcium silicate pieces respectively (EN 771-1 [44] and EN 771-2 [45]). This consideration enables the T1 series mortars and V4T2, V4T5 and V5T2 to perform prefabricated pieces and their application as masonry units. Furthermore, following the RILEM LC2 functional classification of lightweight concretes [46], the mortars presented here can be classified as Class II for construction and isolation applications and in Class III only with isolation purposes.

i) Damping properties

The high damping ratio suggests that this material can be applied in soleplates where impact isolation is needed. The minimum strength required in construction applications according to EN 998-2 [47] is 2.5MPa, and styrofoam and similar materials are usually applied for this purpose. It is possible to reach out extra impact isolation by replacing conventional mortar by aerated cement rubber composites.

ii) Thermal Conductivity

In order to save energy in buildings, materials with low thermal conductivity are required to reduce the heat transfer coefficient U, as is required in different building codes. The Table 8 summarizes the computation of the heat transfer U following the procedure described in EN ISO 6946 [48], for the case of application of V6T5 as construction material in a typical roofing case. After computation the U-value was found 0.47 W/m^2K. As comparison, using plain concrete (λ=1.50 W/(m.K)) instead of V6T5, we obtain a U-value of 0.57 W/m^2K.

Table 8. Computation of the U-value following EN ISO 6946 for a roofing case.

iii) Absorption and water permeability

Their pervious characteristics are interesting to drain and to capture storm water. This is a new application that should be studied due to the intrinsic porosity of cement based materials containing rubber aggregates. This kind of material can be interesting in pavements and as roofing material, to profit water sources and recharging groundwater [49].

5. Conclusions

Although air entrained rubberized mortar is relegated to non-structural applications, it presents both environmental and economic benefits. Being a waste, we can obtain a secondary raw material with added value, diminishing the impact of dumps and landfills, and it can provide energy savings thanks to its low thermal conductivity since it can be used in various construction types as a thermal insulator.

Given the properties of the material used in this study, its application is appropriate as construction material where thermal, acoustic and anti-impact properties are required.

The mortars with superior resistance to 2.5 MPa can also be used as masonry pieces, providing the additional features mentioned. Finally, while we have a society dependent on the use of tires for economic development, we also have a secondary raw material usable in cement based materials.

6. Acknowledgements

The authors appreciate the contribution to this work by Celia Silvestre and Juan Vicente Sabater (AIDICO, Technological Institute of Construction) for providing thermal conductivity results.

7. References

[1] Sistema integrado de gestión de neumáticos usados (SIGNUS). Activity Report 2011. (website): http://www.signus.es/LinkClick.aspx?fileticket=Mn7edNFMSHo%3d&tabid=118. Accessed: February 1, 2013.

[2] Eldin NN, Senouci AB. Rubber-tire particles as concrete aggregate. J Mater Civ Eng 1993; 5: 478-96.

[3] Fattuhi, NI, Clark LA. Cement-based materials containing shredded scrap truck tyre rubber. Constr Build Mater 1996; 10(4): 229-36.

[4] Khatib ZK, Bayomy FM. Rubberized Portland cement concrete. J Mat Civ Eng 1999; 11(3), 206-13.

[5] Raghavan D, Huynh H, Ferraris CF. Workability, mechanical properties, and chemical stability of a recycled tyre rubber filled cementitious composite. J Mat Sci 1998; 33: 1745-52.

[6] Benazzouk A, Douzane O, Langlet T, Mezreb K, Roucoult JM, Quéneudec M. Physico-mechanical properties and water absorption of cement composite

containing shredded rubber wastes. Cem Concr Compos 2007; 29, 732-40.

[7] Fedroff D, Ahmed S, Savas BZ. Mechanical properties of concrete with ground waste tire rubber. J Transp Res Board 1996; 1532: 66–72.

[8] Turatsinze A, Bonnet S, Granju J. Mechanical characterisation of cement-based mortar incorporating rubber aggregates from recycled worn tyres. Build Environ 2005; 40(2): 221-6.

[9] Khaloo AR, Dehestani M, Rahmatabadi P. Mechanical properties of concrete containing a high volumen of tire-rubber particles. Waste Manag 2008; 28: 2472-82.

[10] Siddique R, Naik TR. Properties of concrete containing scrap-tire rubber. An overview. Waste Manag 2004; 24: 563-9.

[11] Rostami H, Zandi I, Silverstrim T. Recycling of Waste Tire in Concrete. Concr 2000 Int Conf Concr Technol 1993, Dundee, Scotland, 391-9.

[12] Segre N, Joekes I. Use of tire rubber particles as addition to cement paste. Cem Concr Res 2000; 30: 1421-5.

[13] Albano C, Camacho N, Reyes J, Feliu JL, Hernández M. Influence of scrap rubber addition to Portland I concrete composites: Destructive and non-destructive testing. Compos Struct 2005; 71: 439-46.

[14] Li G, Stubblefield MA, Garrick G, Eggers J, Abadie C, Huang B. Development of waste tire modified concrete. Cem Concr Res 2004; 34: 2283-9.

[15] Benazzouk A, Douzane O, Mezreb K, Laidoudi B, Quéneudec M. Thermal conductivity of cement composites containing rubber waste particles: Experimental study and modelling. Constr Build mater 2008; 22: 573-9.

[16] Paine KA, Moroney RC, Dhir RK, Application of granulated rubber to improve thermal efficiency of concrete. In: Limbachiya MC, Roberts JJ editors.

Sustainable waste management and recycling: Used/ Post-consumer tyres, London: Thomas Telford; 2004, 179-85.

[17] Sukkontasukkul P. Use of crumb rubber to improve thermal and sound properties of pre-cast concrete panel. Constr Build Mater 2009; 23: 1084-92.

[18] Savas BZ, Ahmad S, Fedroff D. Freeze-Thaw Durability of Concrete with Ground Waste Tire Rubber. J Transp Res Board 1997; 1574: 80-8.

[19] Oikonomou N, Mavridou S. Improvement of chloride ion penetration resistance in cement mortars modified with rubber from worn automobile tires. Cem Concr Compos 2009; 31: 403–7.

[20] Topçu IB, Avcular N. Collision behaviours of rubberized concrete. Cem Concr Res 1997; 27(12): 1893-8.

[21] Hernández-Olivares F, Barluenga G. Fire performance of recycled rubber-filled high-strength concrete. Cem Concr Res 2004. 34(1): 109-17.

[22] Najim KB, Hall MR. A review of the fresh/hardened properties and applications for plain (PRC) and self-compacting rubberized concrete (SCRC). Constr Build Mater 2010; 24: 2043-51.

[23] Benazzzouk A, Douzane O, Mezreb K, Quéneudec M. Physico-mechanical properties of aerated cement composites containing shredded rubber waste. Cem Concr Compos 2006; 28: 650-7.

[24] EN 196-1:2005. Methods of testing cement. Determination of strength.

[25] EN 1015-3:1999. Methods of test for mortar for masonry. Determination of consistence of fresh mortar (by flow table).

[26] ASTM C597-09. Standard Test Method for Pulse Velocity Through Concrete.

[27] ASTM C215-08. Standard Test Method for Fundamental Transverse, Longitudinal, and Torsional Frequencies of Concrete Specimens.

[28] Toutanji HA. The use of rubber tire particles in concrete to replace mineral aggregates. Cem Concr Compos 1996; 18(2): 135-9.

[29] INSTRON Blue Hill, Calculation Reference (website): http://www.instron.com.es/wa/library/StreamFile.aspx?doc=631. Accessed: May 20, 2013.

[30] Turki M, Bretagne E, Rouis MJ, Quéneudec M. Microstructure, physical and mechanical properties of mortar-rubber aggregates mixtures. Constr Build Mater 2009; 23: 2715-22.

[31] Lyndon FD, Balandran RV. Some observations on elastic properties of plain concrete. Cem Concr Res 1986; 16 (3): 314-24.

[32] Malhorta VM, Carino NJ. Handbook on nondestructive testing of concrete, West Conshohocken, PA (USA): ASTM International, CRC Press; 2004.

[33] Landau LD, Lifshitz EM. Teoria de la elasticidad. Volumen 7. Barcelona (Spain): Ed. Reverté; 1982.

[34] Gorisse F. Ensayo y control de los hormigones. Barcelona (Spain): Ed. Técnicos asociados; 1980.

[35] Kriker A, Debicki G, Bali A, Khenfer MM, Chabannet M. Mechanical properties of date palm fibres and concrete reinforced with date palm fibres in hot-dry climate. Cem Concr Compos 2005; 27: 554-64.

[36] Yan L, Jenkins CH, Pendleton RL. Polyolefin fiber-reinforced concrete composites Part I. Damping and frequency characteristics. Cem Concr Res 2000; 30(3): 391–401.

[37] Zheng L, Sharon Huo X,Yuan Y. Experimental investigation on dynamic properties of rubberized concrete. Constr Build Mater 2008; 22: 939–47.

[38] Eiras Fernández JN. Diseño de mezclas cementantes con residuos de neumáticos para la obtención de materiales ligeros y aislantes. Master thesis

2010. Universitat Politècnica de València.

[39] Najim KB, Hall MR. Mechanical and dynamic properties of self-compacting crumb rubber modified concrete. Constr Build Mater 2012; 27(1): 521–30.

[40] Laidoudi B, Marmoret L, Quéneudec M. Reuse of rubber waste in cementitious composites: Hygrothermal behaviour. In: Limbachiya MC, Roberts JJ editors. Sustainable waste management and recycling: Used/ Post-consumer tyres, London: Thomas Telford; 2004, 171-8.

[41] Yaşar E, Erdoğan H, Güneyli H. Determination of the thermal conductivity from physico-mechanical properties. Bull Eng Geol Environ 2008; 67: 219-25.

[42] Hall MR, Najim KB, Hopfe CJ. Transient thermal behaviour of crumb rubber-modified concrete and implications for thermal response and energy efficiency in buildings. Applied Thermal Engineering 2012; 33-34: 77-85.

[43] LIDER v1.0 (Software). Ministerio de fomento, secretaria de estado de vivienda y actuaciones urbanas, 2009. (website): http://www.codigotecnico.org/web/recursos/aplicaciones/contenido/texto_0002.html. Accessed: November 29, 2009.

[44] EN 771-1:2011. Specification for masonry units. Clay masonry units.

[45] EN 771-2:2011. Specification for masonry units. Calcium silicate masonry units.

[46] RILEM LC2. Méthodes d'essais des bétons cellulaires. Mater Constr 1974; 8(45): 224.

[47] EN 998-2:2010. Specification for mortar for masonry . Masonry mortar.

[48] EN ISO 6946:2007. Building components and building elements. Thermal resistance and thermal transmittance. Calculation method.

[49] Tennis PD, Leming ML, Akers DJ. Pervious Concrete Pavements. EB302

Portland Cement Association Skokie IL, and National Ready Mixed Concrete Association; 2004. (website): http://myscmap.sc.gov/marine/NERR/pdf/PerviousConcrete_pavements.pdf. Accessed: February 14, 2013.